Title

Development of a Simple and Reproducible Cell-derived Orthotopic Xenograft Murine Model for Neuroblastoma

Journal

In Vivo, 38(2)

ISSN

0258-851X

Authors

Doyle, Kathleen

Hassan, Abd-Elrahman

Sutter, Maria

et al.

Publication Date

2024

DOI

10.21873/invivo.13471

Peer reviewed

in vivo *38*: 531-538 (2024)
doi:10.21873/invivo.13471

Development of a Simple and Reproducible Cell-derived Orthotopic Xenograft Murine Model for Neuroblastoma

KATHLEEN DOYLE[1], ABD-ELRAHMAN HASSAN[1], MARIA SUTTER[2], MONICA RODRIGUEZ[2], PRIYADARSINI KUMAR[2] and ERIN BROWN[3]

[1]*Department of Surgery, University of California-Davis, Sacramento, CA, U.S.A.;*
[2]*Center for Surgical Bioengineering, Department of Surgery, University of California-Davis, Sacramento, CA, U.S.A.;*
[3]*Department of Surgery, Division of Pediatric Surgery, University of California-Davis, Sacramento, CA, U.S.A.*

Abstract. *Background/Aim: Neuroblastoma is a common childhood cancer with poor survival for children with high-risk disease, and ongoing research to improve outcomes is needed. Patient-derived xenografts (PDX) and genetically engineered mouse models (GEMM) are reliable models for oncologic research; however, they are resource-intensive, expensive, and require significant expertise to develop and maintain. We developed an orthotopic xenograft murine model of neuroblastoma that utilizes cryopreserved banks of human neuroblastoma cell lines, requires minimal equipment, and is easily reproducible. Materials and Methods: The neuroblastoma cell line NB1643 was obtained from the Children's Oncology Group (COG) Childhood Cancer Repository. Nod-SCID-gamma (NSG) mice underwent orthotopic injection of $2x10^6$ NB1643 cells suspended in 10 μl of collagen hydrogel directly into the adrenal gland via an open retroperitoneal surgical approach. Mice were monitored by ultrasound and in vivo imaging system (IVIS) until the tumor reached the volume of the ipsilateral kidney. Tumor identity was confirmed by necropsy and histologic analysis. Results: A total of 55 mice underwent surgery. Eight died due to anesthetic or surgical complications. 39/47 (78%) survivors grew primary adrenal tumors. Average anesthesia time was 30 min. Ultrasound and IVIS successfully characterized tumor growth in all mice. Average time to target tumor size was 5 weeks (range=3-9). Gross pathologic and histologic analysis confirmed adrenal tumors consistent with neuroblastoma in all mice with adrenal masses. Conclusion: A cell-derived orthotopic xenograft murine model can be successfully used to create an in vivo model of neuroblastoma. This model can be utilized in environments where PDX or GEMM models are not feasible.*

Correspondence to: Dr. Kathleen Doyle, MD, Department of Surgery, University of California Davis Medical Center, 2335 Stockton Blvd, North Addition 5th floor, Sacramento, CA 95817, U.S.A. Tel: +1 9167342816, e-mail: kedoyle@ucdavis.edu

Key Words: Neuroblastoma, orthotopic murine model, PDOX.

Neuroblastoma is the most common extracranial solid tumor in children under the age of five and accounts for 15% of cancer-related deaths in children (1). Despite intensive multimodal therapies, high-risk neuroblastoma still carries a 5-year survival rate of <50% (1, 2). Despite decades of research, there has been minimal improvement in the overall survival for children with advanced disease; furthermore, children who do survive often experience long-term disabilities from their treatment. Therefore, the development of new therapies for patients with high-risk disease remains a high priority in order to improve outcomes for children with neuroblastoma (3).

Oncology research relies on reproducible and accurate disease models. Animal xenografts are an essential component of oncologic research as they provide a more accurate representation of the tumor microenvironment compared to *in vitro* models. These models are critical for studying tumor biological features, tumor behavior, preclinical drug screening, assessing treatment response, and development of drug resistance (4, 5). In heterogenous diseases, such as high-risk neuroblastoma, xenograft models can facilitate treatment response across different tumor phenotypes and assess for varied treatment responses (5, 6). However, animal models can be resource intensive to create, often requiring significant expertise and expensive equipment to develop.

We developed a cell-derived orthotopic xenograft murine model for neuroblastoma that is simple, reliable, and easily reproducible. Here we describe the development of our

model, including the procedural steps and tumor monitoring process, the pitfalls and lessons learned during model development, and the overall outcomes of tumor development utilizing this model.

Materials and Methods

Neuroblastoma cell culture. Human neuroblastoma cell line NB1643 was derived from a patient with high-risk disease and obtained from the Children's Oncology Group (COG) cell repository. Cells were cultured in medium containing Iscove's modified Dulbecco's medium (IMDM) (Thermo Fisher Scientific, Waltham, MA, USA), 20% fetal bovine serum (FBS) (Biotechne, Minneapolis, MN, USA), and 1% Insulin-Transferrin-Selenium (ITS-G 100X) (Gibco, Thermo Fisher Scientific), 100 U/ml penicillin and 100 μg/ml streptomycin at 37˚C, 5% CO_2.

Neuroblastoma cell lentiviral transduction. To allow for visualization of tumor cells *via* an *in vitro* imaging system (Lago X, Spectral Instruments Imaging, Tucson, AZ, USA), neuroblastoma cells were transduced with a Luciferase-GFP-Neomycin carrying lentiviral vector. The viral vector (pCCLc-MNDU3-LUC-PGK-EGFP-E2A-Neo-Wpre) was obtained from the UC Davis Vector Core at the Institute for Regenerative Cures, Sacramento, CA, USA. Cells were seeded at a density of 0.25×10^6 cells/well in a 24 well plate and grown overnight. The following day, lentivirus was added to cells at a multiplicity of infection (MOI) of 10 for an incubation period of 24 h. Transduction medium consisted of IMDM and 8 μg/ml protamine sulfate. After incubation, cells were washed twice with PBS and the use of normal culture medium was resumed. Cells were then expanded for 48-72 h, and successful transduction was observed by fluorescence microscopy using inverted microscopy (a Carl Zeiss Axio Observer D1, Zeiss Group, Jena, Germany). Transduced cells were selected for using a dose of 600 μg/ml Geneticin (Gibco, Thermo Fisher Scientific) for 1 week. Cells were then expanded and stored.

Murine preparation. All studies were approved by the Institutional Animal Care and Use Committee (IACUC) at UC Davis Medical Center. All animals were maintained in a pathogen-free environment in the animal vivarium facility at UC Davis Medical Center Sacramento Campus. Nod-SCID-gamma (NSG) mice (Jackson Laboratory, Sacramento, CA, USA) age 6-8 weeks were used. Equal numbers of male and female mice were used (27 females and 28 males).

Surgical technique. General anesthesia was induced with 2% isoflurane gas. Mice were placed on the operating table in the prone position and limbs and tail were secured. Anesthesia was maintained *via* nosecone delivering 2% isoflurane. A 1-cm vertical skin incision was made over the left upper back approximately 1cm caudad and lateral to the most convex portion of the murine spinal column (Figure 1). The retroperitoneum was opened with a small <0.5 cm incision over the kidney using visualization of the kidney through the retroperitoneal fat to guide incision location. The retroperitoneum was visually explored to identify the position of the kidney, extending the incision to a total length of 1cm directly over the kidney. Care was taken to ensure that the incision did not extend too far cephalad to avoid diaphragmatic injury.

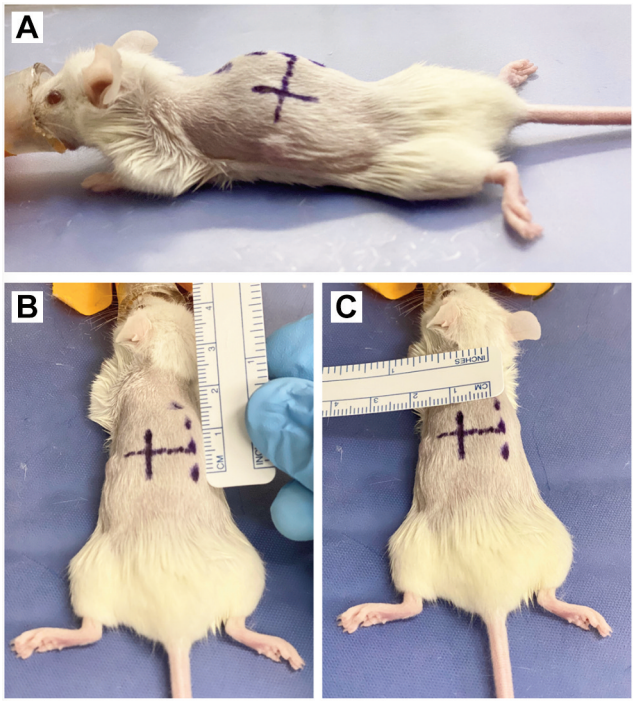

Figure 1. *Incision location. (A) Mouse spinal column convexity (dotted line) is primary anatomical landmark for incision location. Crossed solid lines represent incision location: 1 cm caudal from the most convex portion of the spinal column and one cm lateral and to the left of the midline. (B) Incision length is 1 cm and made in the cephalad to caudad direction. (C) Incision is 1 cm lateral and to the left to midline.*

Blunt dissection was used to separate the retroperitoneal fat from the kidney and to retract the left lobe of the liver and spleen laterally and cephalad. The adrenal gland and fat pad were identified and brought into the operative field with gentle blunt retraction of the kidney, retraction of the skin and retroperitoneal fat with forceps (Figure 2). The primary surgeon (seated at the tail side of the mouse) used their non-dominant hand to stabilize the kidney and visualize the adrenal gland. The assistant surgeon (seated at the head side of the mouse) retracted the skin and retroperitoneal fat. Under direct visualization, the operating surgeon then injected 2×10^6 of NB1643 cells suspended in 10 μl of collagen hydrogel into the adrenal gland and surrounding fat pad (Figure 3). The wound was closed in two layers (retroperitoneum and skin) with absorbable suture in a running fashion. Mice were recovered from anesthesia and observed for a minimum of fifteen minutes prior to returning to the vivarium.

Post-operative monitoring was performed with daily weights for 7 days. Pain medications were administered for 48 h after surgery. Mice were singly housed until their surgical incisions healed (average of 7 days). Sutures were removed 7-10 days after surgery per policy.

Tumor monitoring. Tumors growth was monitored with bioluminescence utilizing IVIS (IVIS, Lago X, Spectral Instruments) (Figure 4). Mice were injected with luciferin solution [injection volume (ml)=weight (g)×10] *via* intraperitoneal injection

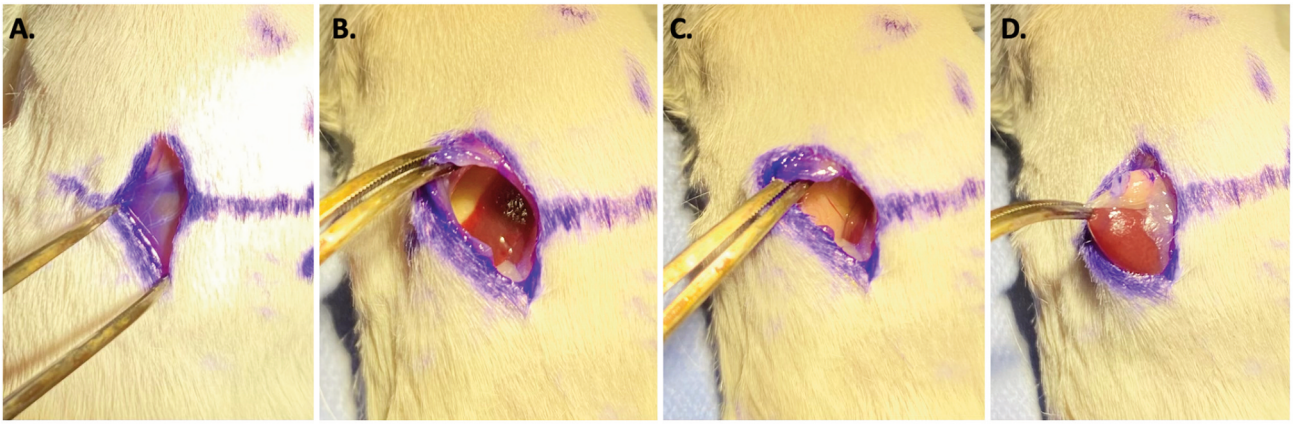

Figure 2. *Surgical technique. (A) The incision was made through the skin. Image demonstrates retroperitoneal fat plane that is encountered after skin incision. Through the retroperitoneal fat the kidney can be visualized to ensure the incision is not too low or too high. (B) After incision through the retroperitoneum the left lobe of the liver is often encountered. (C) The left lobe of the liver should be bluntly and gently retracted cephalad and lateral to expose the kidney, which is shown on the right side of the incision here. (D) the adrenal gland is exposed. The adrenal gland can be gently brought into the incision by grasping the surrounding fat pad to avoid injury to the adrenal gland or kidney.*

using a 27-gauge needle and were then placed under general anesthesia. IVIS imaging was performed 10 min post-injection with bioluminescent imaging settings in both the dorsal and ventral position followed weekly.

Tumor growth was also monitored with ultrasound (Wilsonic Piloter Veterinary ultrasound, Core Imaging, Grand Rapids, MI, USA) using 6-15 MHz hockey stick probe. Mice underwent general anesthesia and tumor volume measurements were taken weekly until the tumor was 0.5-1× the size of the ipsilateral kidney. Mice were monitored for a maximum of 12 weeks at which point mice were euthanized and necropsy performed (Figure 5).

Histologic analysis. At the time of necropsy, whole tumors were fixed in 10% formalin for 24 h and then transitioned to sucrose solution. Specimens were sectioned and stained with hematoxylin and eosin (H&E) and compared to human neuroblastoma samples for diagnostic confirmation. Additional organs (liver, spleen, lung, vertebral column) and any gross evidence of metastatic disease were also collected and sectioned to evaluate for metastatic lesions.

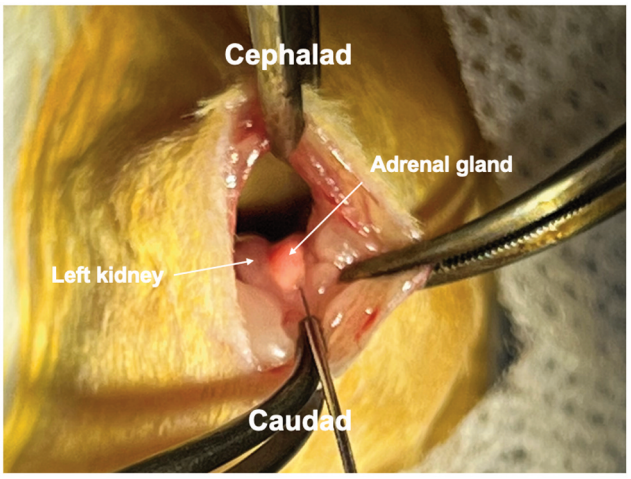

Figure 3. *Injection of neuroblastoma cells. Image showing the syringe containing neuroblastoma cells directly being injected into the left adrenal gland.*

Results

A total of 55 mice underwent surgery. Eight mice died from surgical or anesthetic complications prior to established tumor growth and were excluded from further analysis (Figure 6). Initial operative times was 60 min from induction of anesthesia to anesthetic recovery. As the study progressed, operative time decreased to fifteen minutes, with time to adrenal exposure ranging from 2 to 5 min from skin incision. Incision size was initially 1.5 to 2 cm but decreased to 1 cm or less over the course of model development.

Of the 47 mice that survived, 39 mice grew primary adrenal tumors (83%), 3 mice (6.3%) grew non-adrenal tumors (2 with liver lesions, 1 with mesenteric lesions), and 5 mice (10.6%) had no tumors (Figure 7). Of note, 4 out of 5 mice that did not grow tumors were from the first round of surgeries likely due to difficulty with injection technique and lack of appropriate cell delivery. Similarly, the mice with liver and mesenteric lesions were likely related to difficulty maintaining a neuroblastoma cell pellet within the adrenal gland and surrounding fat pad. We transitioned to use of 10 µl of collagen hydrogel for neuroblastoma cell injection with significant improvement in our overall engraftment rate from 50% during the first round of surgery to 100% in our last round of surgical model creation. The adrenal tumors were large and often exhibited evidence of invasion into surrounding structures such as the kidney and

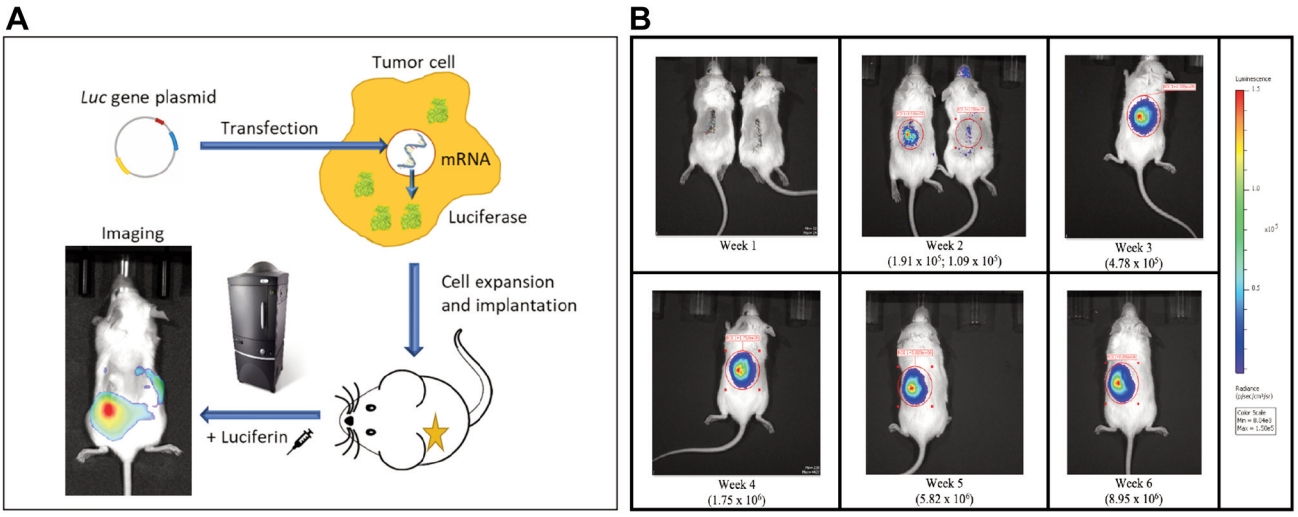

Figure 4. *In vivo imaging system monitoring of tumor growth. (A) Schematic for mechanism of bioluminescent imaging via IVIS. Neuroblastoma cells (NB1643) were transfected with luciferase gene via plasmid. Mice were injected with luciferin and a bioluminescent signal was emitted and measured by IVIS machine. (B) Serial weekly images demonstrating presence of neuroblastoma cells in the mouse and then coalescence of the cell signal to the left adrenal gland as the tumor grows and develops. IVIS: In vivo imaging system.*

diaphragm. No mice with adrenal tumors exhibited evidence of metastatic disease.

Three mice experienced post-operative wound dehiscence requiring reoperation. In these cases, superficial wound dehiscence occurred on post-operative days 1-4; there was no violation of the retroperitoneum, and the wounds cleansed and reapproximated. Two mice recovered well and completed the study, while one required euthanasia due to failure to heal. Use of monofilament sutures improved wound healing over the study period. No other post-operative complications occurred.

Both IVIS and US imaging successfully monitored tumor growth and development. Over time, bioluminescent signals strengthened and became more concentrated over the left adrenal gland, corresponding to tumor location (Figure 4). Average time to tumor visualization on US was 5 weeks (range=3-9). Average time to target tumor size was approximately 6 weeks (Figure 8). H&E staining for all tumors demonstrated small, round blue cells characteristic of neuroblastoma (Figure 9).

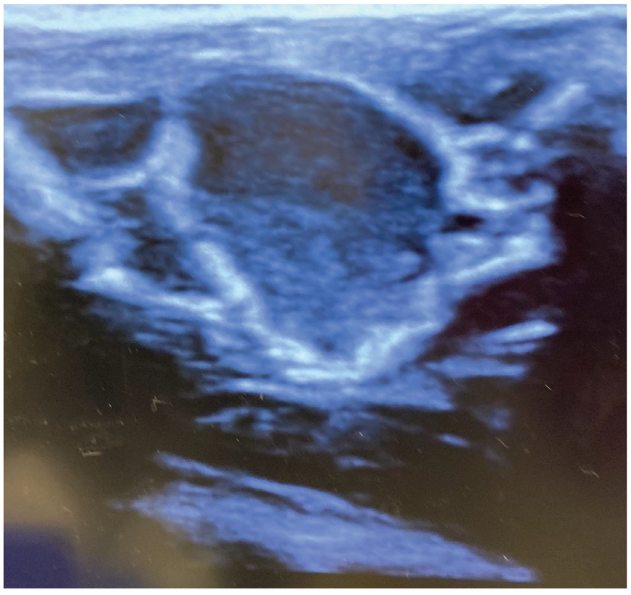

Figure 5. *Tumor image on ultrasound. Five weeks post NB cell injection. Diameter: 0.79 cm and area: 0.40 cm^2. NB: Neuroblastoma.*

Discussion

We successfully developed a cell-derived orthotopic xenograft model for neuroblastoma that is simple and reliable utilizing relatively low-cost ultrasound and anesthetic equipment. After the initial learning curve associated with model development, tumor engraftment rates approached 100% and operative times decreased from 60 to 15 min. We describe a reliable surgical model for neuroblastoma with high engraftment rates and review the current neuroblastoma models available for research in this important field.

Significant pitfalls during model creation included too much manipulation of abdominal viscera, which led to longer surgeries and more trauma to the animal. Incision placement was critical to avoid surgical complications. An

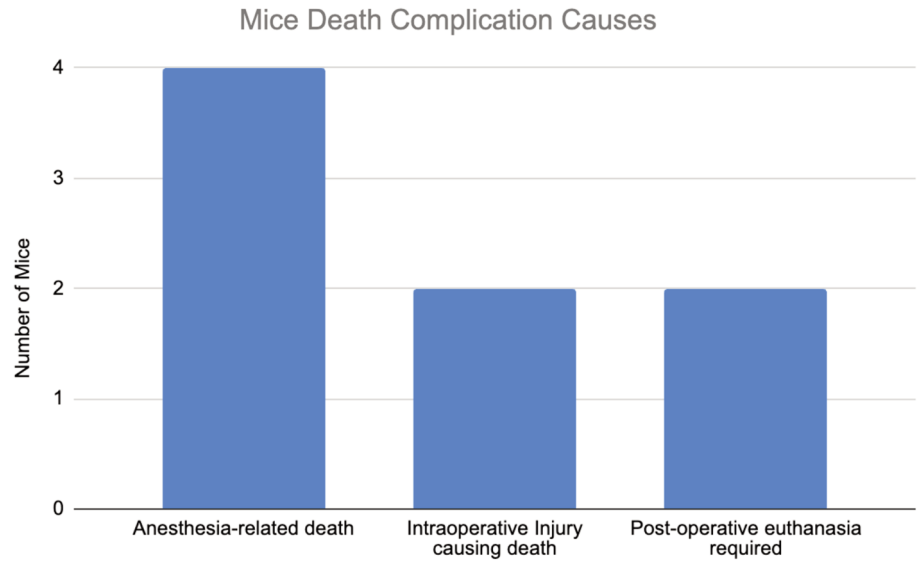

Figure 6. *Complications leading to murine death prior to tumor development. Four mice died from anesthetic complications during surgery or post-operative imaging. Two mice had intraoperative injuries that resulted in death. Two mice required post-operative euthanasia for reasons unrelated to surgery (one mouse had a self-inflicted tail injury requiring euthanasia and one mouse was found to have been injected with neuroblastoma cells contaminated with mycoplasma).*

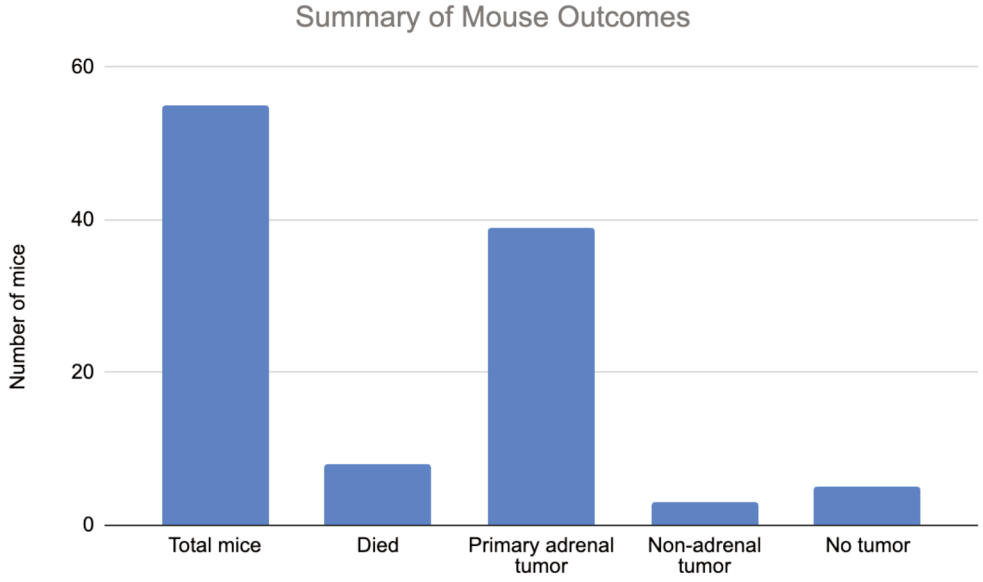

Figure 7. *Summary of mouse outcomes. A total of 55 mice underwent surgery. Eight died due to surgical or anesthetic complications. Thirty-nine mice grew primary adrenal tumors resulting in an engraftment rate of 83%. Three mice had non-adrenal lesions. Five mice had no tumor growth.*

incision placed too high risks injury to the diaphragm, which results in a fatal injury in a mouse model. An incision placed too low can be complicated by colonic injury. After skin incision, landmarks such as the left lobe of the liver or even the left kidney are identified through the retroperitoneal fat pad to guide our retroperitoneal incision, minimized the length of the overall incision. Careful and minimal retraction of the liver and spleen is necessary as both are easily injured from excessive force or instrument manipulation. Improvements in cell injection technique and the use of collagen hydrogel also significantly improved the overall success of the model. Overall, the model was successfully

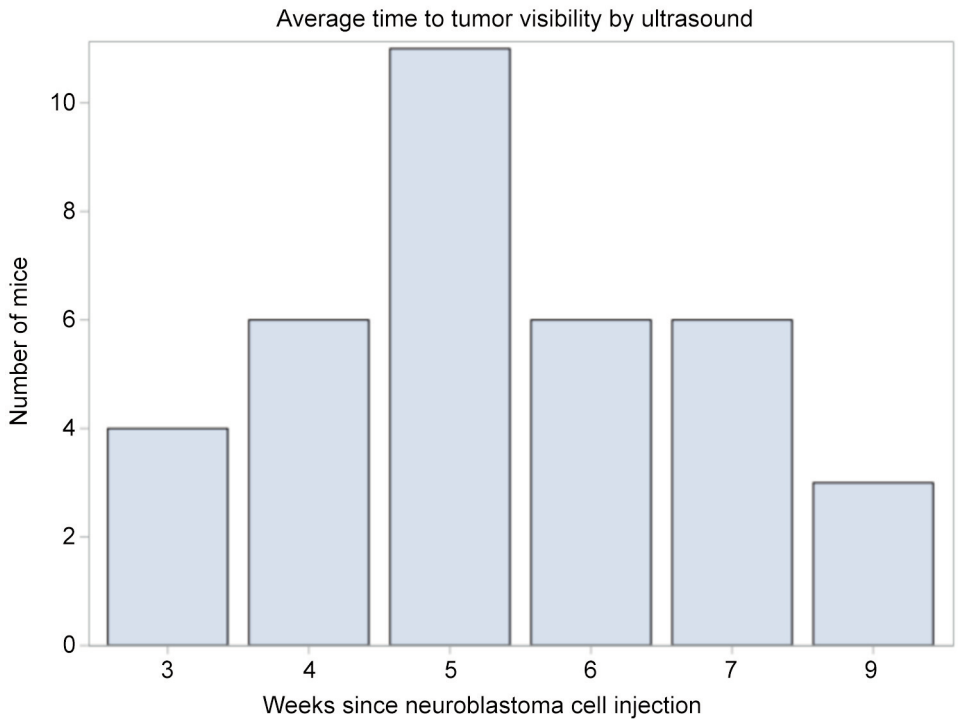

Figure 8. *Weeks to tumor visibility on ultrasound from time of neuroblastoma cell injection. Average time was 5 weeks with a range of 3-9 weeks.*

developed in a short period of time, even when accounting for the initial learning curve of model creation.

While IVIS equipment may not be feasible for all scientific investigators, we also monitored tumor growth with ultrasound using a Wisonic Piloter Veterinary ultrasound 6-15 MHz probe. This model has less resolution than the 22-55 MHz probes described in the literature (4, 7) and is notably less expensive and more widely available. Multiple studies have demonstrated the successful use of ultrasound for monitoring tumor growth *in vivo*, with equal or superior outcomes compared to bioluminescence imaging alone (4, 8). There was no significant difference in the imaging capability of IVIS compared to US. In fact, US monitoring facilitating more accurate tumor identification and measurement over time. For these reasons, our lab has transitioned to exclusive ultrasound monitoring for current studies, making this model more accessible to researchers without IVIS capabilities.

A common oncologic model utilized in the literature is the patient-derived xenograft (PDX) model. In this model, fresh primary or metastatic patient tumor tissue are implanted into the mouse in either a heterotopic or orthotopic manor (5). The tumor can then be grown, harvested, and expanded in multiple mice. This approach most accurately mimics the tumor microenvironment and allows for modeling of real patient tumors and quick model expansion for studying real time tumor behaviors and drug response/resistance (5, 6, 9, 12). In contrast to a heterotopic model where the tumor is grown in a non-native location, an orthotopic model (PDOX) allows for better simulation of the real tumor biology and behavior (5, 6, 9, 12). However, patient-derived orthotopic xenografts (PDOX) models

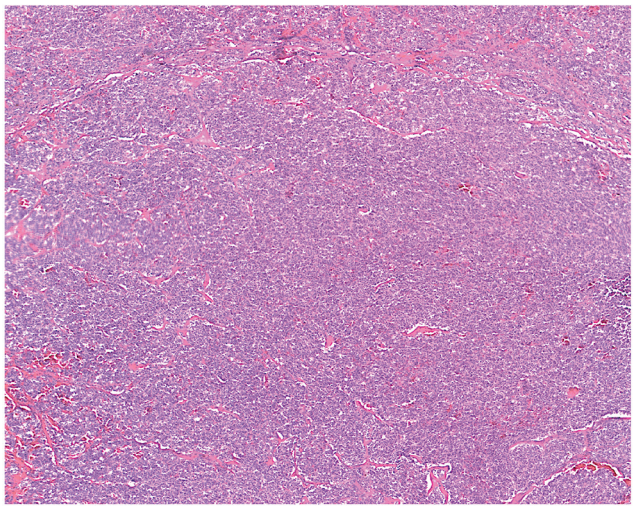

Figure 9. *Histology results. Hematoxylin and eosin (H&E) staining of adrenal tumor (20×). Sample demonstrates small, round, blue cells consistent with neuroblastoma.*

require specific expertise and resources that may not be readily available for all groups. Specifically, PDOX requires a functioning biorepository that can store and process patient specimens in real time as well as a team trained in PDOX creation that is available for immediate implantation following specimen processing. Lastly, a shortcoming of both the PDOX model and the model described in this study is the requirement for immunosuppressed mice to allow for tumor growth (6). This limits the ability of immunotherapy testing and may not accurately represent the natural tumor microenvironment. However, PDOX models have been shown to parallel clinical outcome in various tumor types, including neuroblastoma and are the current gold standard for neuroblastoma research (5, 6).

An alternative to the orthotopic models is a genetically engineered mouse model (GEMM). GEMM requires gene-editing to breed mice with the desired tumor expression. There are a multitude of GEMM models including oncogene knock-ins, tumor suppressor knockouts, and even models that can mimic somatic mutations seen more commonly in spontaneously occurring adult tumors (10-12). GEMM develop *de novo* tumors in a natural immune-proficient microenvironment. These tumors retain the histopathological and molecular features of real human tumors, as well as display the genetic heterogeneity and tendency for metastatic spread (10-12). In neuroblastoma specifically, the TH-MYCN murine model is the most common GEMM. These transgenic mice were created to overexpress N-MYC in neural crest cells under control of rat tyrosine hydroxylase (TH) promoter (13). In GEMM, only tumors with known specific genetic alterations can be modeled, which is problematic in neuroblastoma where high-risk disease is markedly heterogeneous and undergoes constant genetic and molecular rearrangements and mutations (14). In general, GEMM are time-consuming, laborious, and expensive to develop and maintain, and as a result, it not a widely available model for all researchers or pilot studies.

A reliable animal model is essential in the current age of research and is especially critical in neuroblastoma for a more comprehensive modeling of human disease and assessment of treatment response. While the PDOX or GEMM may retain histopathological features of neuroblastoma and represent important models for research, they are expensive and resource intensive, and may not be feasible for all laboratories or for pilot studies. Here we have developed and described a model that requires fewer resources and is less expensive than PDOX or GEMM but remains reliable in terms of reproducible neuroblastoma tumor growth. While this model demonstrated locally aggressive tumor features similar to neuroblastoma, distant metastases were not evident. This may be limited by the relatively short time from tumor growth to euthanasia or the specific cell line utilized for model creation. Additionally, we used neuroblastoma cell lines obtained from cell-culture, which are known to less accurately represent the true tumor microenvironment and tumor response to treatment. We also utilized a single cell line, which is not representative of the heterogeneity of neuroblastoma and tumor behavior would likely differs between different cell lines. Models utilizing multiple cell lines to better understand tumor behavior and response to treatment is essential (15), and the current model can be easily translated to other cell lines and alternative cell sources can be utilized with a similar technique. Peritoneal and hepatic injection techniques could be considered to develop a metastatic neuroblastoma model in future studies as evidenced by the liver and peritoneal tumor growth identified early in model creation. Lastly, while we characterized the tumors by histologic staining, more rigorous methods for tumor characterization, such as proteomics, could be pursued as some studies have shown that the xenograft proteome do not necessarily mimic the native tumor proteome (16). Future studies could explore the proteomic differences of xenograft tumors from different sources and how this may influence tumor behavior in a xenograft model. Despite these limitations, we believe that this model offers a reliable and less resource-intensive alternative murine model for neuroblastoma research.

Conclusion

We developed a reliable orthotopic murine model for neuroblastoma utilizing human neuroblastoma cells cultured in a medium and injected directly into the adrenal gland *via* open surgical approach. We believe that this is a model that could be easily reproduced in a variety of settings and does not require many of the expensive resources for other models such as GEMM or PDOX.

Funding

This work is funded by NIH grants 1T32CA251007 (KD) and 2K12CA138464 (EB).

Conflicts of Interest

The Authors have no conflicts of interest to disclose related to the above manuscript.

Authors' Contributions

Authors Doyle, Brown, and Hassan were responsible for developing study concept and design. Authors Sutter, Rodriguez, and Kumar were responsible for cell preparation and transfection. Authors Doyle and Hassan performed all murine surgeries. Authors Sutter, Rodriguez, and Doyle performed histologic analysis. Author Doyle performed data collection, statistical analysis, and primary manuscript drafting and critical review. Authors Brown, Kumar, and Sutter performed critical review of the manuscript.

Acknowledgements

The Authors would like to acknowledge the Surgical Center for Bioengineering at University of California Davis, Sacramento CA for providing laboratory space, equipment, and assistance with elements of model development.

References

1 Hochheuser C, Windt LJ, Kunze NY, de Vos DL, Tytgat GAM, Voermans C, Timmerman I: Mesenchymal stromal cells in neuroblastoma: exploring crosstalk and therapeutic implications. Stem Cells Dev 30(2): 59-78, 2021. DOI: 10.1089/scd.2020.0142

2 Davidoff AM: Neuroblastoma. Semin Pediatr Surg 21(1): 2-14, 2012. DOI: 10.1053/j.sempedsurg.2011.10.009

3 Upton K, Modi A, Patel K, Kendsersky NM, Conkrite KL, Sussman RT, Way GP, Adams RN, Sacks GI, Fortina P, Diskin SJ, Maris JM, Rokita JL: Epigenomic profiling of neuroblastoma cell lines. Sci Data 7(1): 116, 2020. DOI: 10.1038/s41597-020-0458-y

4 VAN Noord RA, Thomas T, Krook M, Chukkapalli S, Hoenerhoff MJ, Dillman JR, Lawlor ER, Opipari VP, Newman EA: Tissue-directed implantation using ultrasound visualization for development of biologically relevant metastatic tumor xenografts. In Vivo 31(5): 779-791, 2017. DOI: 10.21873/invivo.11131

5 Hidalgo M, Amant F, Biankin AV, Budinská E, Byrne AT, Caldas C, Clarke RB, de Jong S, Jonkers J, Mælandsmo GM, Roman-Roman S, Seoane J, Trusolino L, Villanueva A: Patient-derived xenograft models: an emerging platform for translational cancer research. Cancer Discov 4(9): 998-1013, 2014. DOI: 10.1158/2159-8290.CD-14-0001

6 Braekeveldt N, Bexell D: Patient-derived xenografts as preclinical neuroblastoma models. Cell Tissue Res 372(2): 233-243, 2018. DOI: 10.1007/s00441-017-2687-8

7 Jäger W, Moskalev I, Janssen C, Hayashi T, Gust KM, Awrey S, Black PC: Minimally invasive establishment of murine orthotopic bladder xenografts. J Vis Exp (84): e51123, 2014. DOI: 10.3791/51123

8 Teitz T, Stanke JJ, Federico S, Bradley CL, Brennan R, Zhang J, Johnson MD, Sedlacik J, Inoue M, Zhang ZM, Frase S, Rehg JE, Hillenbrand CM, Finkelstein D, Calabrese C, Dyer MA, Lahti JM: Preclinical models for neuroblastoma: establishing a baseline for treatment. PLoS One 6(4): e19133, 2011. DOI: 10.1371/journal.pone.0019133

9 Tian H, Lyu Y, Yang YG, Hu Z: Humanized rodent models for cancer research. Front Oncol 10: 1696, 2020. DOI: 10.3389/fonc.2020.01696

10 Kersten K, de Visser KE, van Miltenburg MH, Jonkers J: Genetically engineered mouse models in oncology research and cancer medicine. EMBO Mol Med 9(2): 137-153, 2017. DOI: 10.15252/emmm.201606857

11 Chesler L, Weiss WA: Genetically engineered murine models—contribution to our understanding of the genetics, molecular pathology and therapeutic targeting of neuroblastoma. Semin Cancer Biol 21(4): 245-255, 2011. DOI: 10.1016/j.semcancer.2011.09.011

12 Kamili A, Atkinson C, Trahair TN, Fletcher JI: Mouse models of high-risk neuroblastoma. Cancer Metastasis Rev 39(1): 261-274, 2020. DOI: 10.1007/s10555-020-09855-0

13 Krawczyk E, Kitlińska J: Preclinical models of neuroblastoma-current status and perspectives. Cancers (Basel) 15(13): 3314, 2023. DOI: 10.3390/cancers15133314

14 Seitz G, Armeanu-Ebinger S, Warmann S, Fuchs J: Animal models of extracranial pediatric solid tumors. Oncol Lett 4(5): 859-864, 2012. DOI: 10.3892/ol.2012.852

15 Kang J, Kamal A, Burrows FJ, Evers BM, Chung DH: Inhibition of neuroblastoma xenograft growth by Hsp90 inhibitors. Anticancer Res 26(3A): 1903-1908, 2006.

16 Tsangaris GT, Dimas K, Malamou A, Katsafadou A, Papathanasiou C, Stravopodis DJ, Vorgias CE, Gazouli M, Anagnostopoulos AK: Molecular proteomic characterization of a pediatric medulloblastoma xenograft. Cancer Genomics Proteomics 14(4): 267-275, 2017. DOI: 10.21873/cgp.20037

Received November 13, 2023
Revised December 24, 2023
Accepted January 5, 2024